ACES

DOI: 10.1002/asia.201500675

CHEMISTRY
AN ASIAN JOURNAL
Full Paper

Biosensors

Catalytic Hairpin Assembly-Programmed DNA Three-Way Junction for Enzyme-Free and Amplified Electrochemical Detection of Target DNA

Shufeng Liu,* Wenji Wei, Tao Liu, and Li Wang*[a]

Abstract: DNA three-way junctions (DNA 3WJ) have been widely used as important building blocks for the construction of DNA architectures and dynamic assemblies. Herein, we describe for the first time a catalytic hairpin assembly-programmed DNA three-way junction (CHA-3WJ) strategy for the enzyme-free and amplified electrochemical detection of target DNA. It takes full advantage of the target-catalyzed hairpin assembly-induced proximity effect of toehold and branch-migration domains for the ingenious execution of the strand displacement reaction to form the DNA 3WJ on the electrode surface. A low detection limit of 0.5 pM with an excellent selectivity was achieved for target DNA detection. The developed CHA-3WJ strategy also offers distinct advantages of simplicity in probe design and biosensor fabrication, as well as enzyme-free operation. Thus, it opens a promising avenue for applications in bioanalysis, design of DNA-responsive devices, and dynamic DNA assemblies.

Introduction

During the past decades, the development of DNA biosensors for the amplified detection of DNA has been continually pursued owing to its potential applications in molecular diagnosis, forensic investigations, genetic therapy, and biomedical development.[1] In order to satisfy the requirement to profile low-abundance target DNA, different signal amplification strategies, especially nuclease-based target recycling strategies, are often used in DNA biosensors.[2] They usually involve the individual or combined use of various nucleases including endonuclease, exonuclease, and polymerase, to achieve recycling of the target itself and/or the concomitant generation of large amounts of target-associated nucleic acid sequences for signal amplification.[3] However, the employment of nucleases may increase the complexity of the experimental system, the assay cost, and even the risk of false-positive signal output for target detection. Thus, the development of enzyme-free signal amplification strategies that allow targets to be profiled with high confidence is highly desirable for diagnostic purposes.

The DNA three-way junction (3WJ) consisting of three complementary oligonucleotide branches has been widely utilized as a building block to construct DNA architectures and dynamic assemblies.[4] It has also been exploited as a scaffold for the controlled arrangement of functional molecules, including a wide range of different chromophores.[5] Target-responsive DNA 3WJs can also be designed into DNA devices for molecular diagnostic, sensing, and imaging applications.[6] The DNA 3WJ strategy for target DNA detection is usually operated via the use of three strands, called assistant DNA, target DNA, and reporter DNA. In the presence of target DNA, hybridization with assistant DNA and reporter DNA is feasible, thereby leading to the formation of DNA 3WJ. Recently, the strategy concerning the binding-induced formation of DNA 3WJ has also been well developed for the detection towards a wide spectrum of analytes, from small molecules and nucleic acids to proteins.[7] Herein, the target binding induces a proximity effect of the two DNA motifs and initiates a subsequent strand displacement, resulting in a binding-induced DNA 3WJ for the signal output toward the bio-recognition or biosensing events. However, the typical DNA 3WJ strategy or the binding-induced DNA 3WJ strategy is often confronted with an unsatisfactory detection performance toward analytes. With the further combination of nuclease-based signal amplification strategies, the sensitivity to analytes could be improved,[8] but the above-referred nuclease issues may also coexist and restrict its wide application to some extent. Also, the DNA 3WJ strategy is more often combined with the fluorescence detection technique. By comparison, an electrochemical method could provide significant advantages, such as simple and portable instrumentation, rapid response, low cost, and high sensitivity. The target-catalyzed hairpin assembly (CHA), as a typical enzyme-free signal amplification strategy, has been widely used for the detection toward various biomolecule targets serving for bio-diagnosis

[a] *Dr. S. Liu, W. Wei, T. Liu, Dr. L. Wang*
Key Laboratory of Sensor Analysis of Tumor Marker
Ministry of Education
College of Chemistry and Molecular Engineering
Qingdao University of Science and Technology
No. 53 Rd. Zhengzhou, Qingdao, Shandong 266042 (China)
E-mail: sliu@qust.edu.cn
wangli@qust.edu.cn

Supporting information for this article is available on the WWW under http://dx.doi.org/10.1002/asia.201500675.

and the biomedical area.[9] It is routinely operated with the catalytic assembly of two DNA hairpins into duplex DNA, accompanied with the cycling use of target for signal amplification. Inspired by the observation that the assembled duplex DNA by the CHA strategy could bring two DNA segments into close proximity and also considering the operation flexibility and signal amplification capability of the CHA, the catalytic hairpin assembly-programmed DNA three-way junction (CHA-3WJ) strategy was conceived to offer a promising avenue for the amplified detection of DNA.

Herein, the CHA-3WJ strategy is proposed for the first time for the enzyme-free and sensitive electrochemical detection of target DNA. It takes full advantage of the CHA-induced proximity effect of toehold and branch-migration domains for the ingenious execution of the target DNA-initiated strand displacement reaction to form DNA 3WJ. In the current electrochemical strategy, the target recognition and signal amplification by the CHA are operated homogenously. Furthermore, the exact execution of CHA for the formation of DNA 3WJ on the electrode guarantees the detection of target DNA with a high confidence and sensitivity.

Results and Discussion

Design of the CHA-3WJ strategy

The proposed CHA-3WJ strategy for the enzyme-free and amplified electrochemical detection of target DNA is schematically illustrated in Figure 1. The target-catalyzed hairpin assembly (CHA) is intrinsically dependent on the toehold-mediated strand displacement reaction.[9d,10] Firstly, target DNA hybridizes with and opens the HP1 by means of a toehold-mediated strand displacement reaction. The opened HP1 could further hybridize with HP2 based on another toehold-mediated strand displacement reaction, accompanied with the release of the target DNA. The displaced target DNA is free to further propagate the assembly of HP1 and HP2. The formed HP1-HP2 hybrids after CHA exactly bring two DNA domains, the protruding DNA segment **a** at the 3′-terminus of HP1 and the caged DNA segment **b** in the stem region of HP2, into close proximity, which then could act as the toehold and branch-migration domain, respectively, to trigger the toehold-mediated strand displacement reaction between HP1-HP2 hybrids and the immobilized hybrids of I-DNA and B-DNA, resulting in the formation of a stable DNA three-way junction (3WJ) on the electrode and the release of B-DNA.[11] The HP2 was labeled with a ferrocene at its 5′-end. Once the DNA 3WJ was formed on the electrode surface, the electrochemical response of ferrocene towards target DNA was achieved. In the absence of target, no HP1-HP2 hybrids were produced. The DNA fragment **b** carrying a ferrocene label at the 5′-terminus of HP2 was still caged in the stem region and the toehold-mediated strand displacement on the electrode would not occur for electrochemical response. Herein, the introduction of CHA for target recognition and the formation DNA 3WJ offers several advantages. First, it could realize the enzyme-free target recycling for the signal amplification toward target DNA detection. Second, the toehold-mediated strand displacement reaction on the electrode depends on the proximity effect of domain **a** in HP1 and domain **b** in HP2, which could be exactly operated by CHA. Third, the ultimate signal generation originates from the hybridization between the domain **b** in the HP2 and domain **b*** in the I-DNA by the strand displacement reaction. These two domains were initially caged by their complementary sequences, which would be beneficial for the reduction of the background signal. It should be noted that, although CHA strategy has been widely used for enzyme-free detection of various biomolecules, its ingenious utility for toehold-mediated strand displacement reaction based on the proximity effect of two functional DNA fragments after hairpin assembly is reported for the first time.

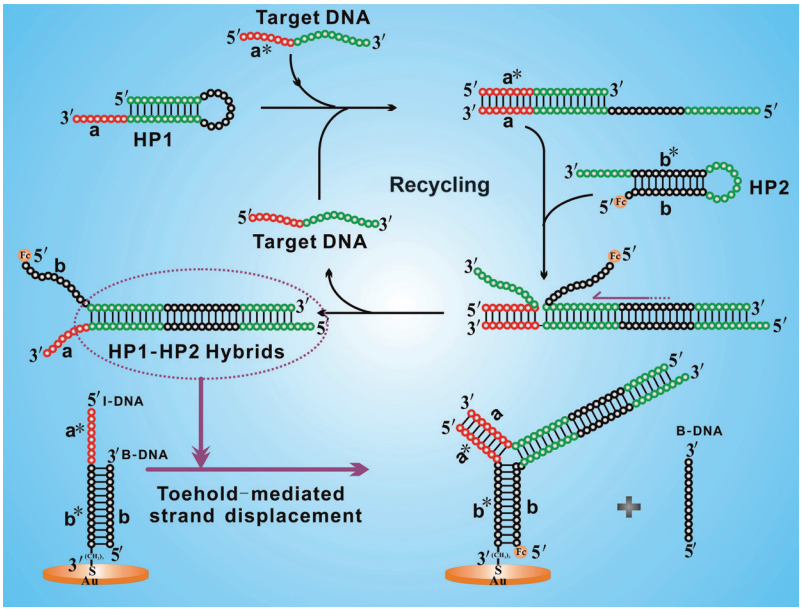

Figure 1. Schematic illustration for target DNA detection based on the CHA-3WJ strategy.

Feasibility of the fabricated DNA biosensor for target DNA detection

The feasibility of the proposed electrochemical biosensor for target DNA detection was firstly verified by using the differential pulse voltammetry (DPV) method (Figure 2A). A readily detectable electrochemical reduction signal of ferrocene at the potential of about 0.2 V was obtained in the presence of target DNA (curve b in Figure 2A). However, only a very weak electrochemical response

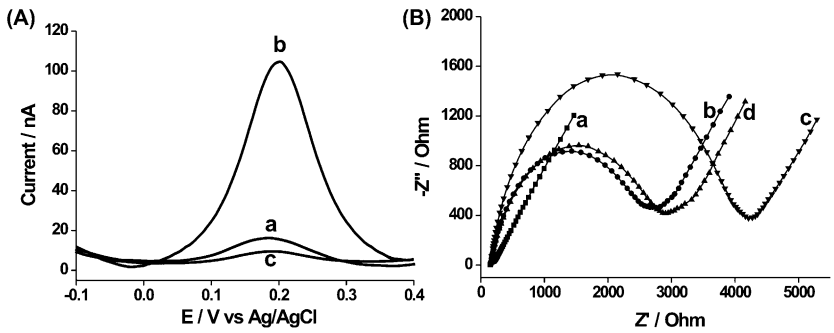

Figure 2. (A) DPV of the electrochemical DNA biosensor. The curves of a and b are the corresponding DPV responses in the absence and presence of 1 nM target DNA, respectively. The curve c corresponds to the DPV response in the presence of target DNA and HP2 but absence of HP1. (B) EIS of the different modified electrodes. The curves were obtained for bare gold electrode (a), the duplex DNA-modified electrode (b), the recognition toward 1 nM target DNA (c), and the control electrode in the absence of target DNA (d), respectively.

could be obtained in the case of absence of target DNA (curve a in Figure 2A). A further decrease of electrochemical response could be obtained for the control experiment operated in the presence of target DNA and HP2 but without HP1 (curve c in Figure 2A), indicating that the direct strand displacement reaction between the caged domain **b** in HP2 and the B-DNA on the electrode surface would hardly occur. The DPV experiments could strongly verify the response mechanism of the CHA-induced toehold-mediated strand displacement reaction for the formation of DNA 3WJ on the electrode surface. The electrode modification and biosensor fabrication was also confirmed by electrochemical impedance spectroscopy (EIS) measurements (Figure 2B). An almost straight line was observed for the bare gold electrode (curve a in Figure 2B), which is a typical characteristic of a mass diffusion-controlled electrode transfer process. Nevertheless, after assembly of the duplex DNA on the electrode, a big semicircle with a charge-transfer resistance (R_{ct}) value of about 2695 Ω could be observed (curve b in Figure 2B), indicating an evident increase of the charge-transfer resistance, which could be ascribed to the repulsion of the negatively charged redox species, $Fe(CN)_6^{3-/4-}$ from approaching the electrode surface by the negatively charged phosphate backbone of duplex DNA. After the CHA-induced strand displacement reaction, the diameter of the semicircle evidently increased, with a R_{ct} value of about 4247 Ω (curve c in Figure 2B), which could be understood in such a way that the formed DNA 3WJ on the electrode after the CHA-induced strand displacement reaction increased the negative charge of the electrode interface for a decreased interfacial charge transfer. It should be noted that the R_{ct} value was only slightly increased in the absence of target DNA compared with that of the duplex probe-modified electrode (curve d in Figure 2B). Thus, the EIS experiments lend further support for the biosensor fabrication process by the CHA-3WJ strategy.

We also synthesized two single-stranded DNAs (S1 and S2) that contained the toehold and branch-migration domain, respectively. The dsDNA hybrids formed by S1 and S2 could be used as a substitute of HP1-HP2 hybrids. The electrochemical responses could be found at two different concentrations of dsDNA hybrids (Figure S1, Supporting Information), thus providing further evidence that the electrochemical response was indeed initiated by the toehold-mediated strand displacement reaction on the electrode surface. The feasibility of the proposed CHA-3WJ strategy for target DNA detection was further verified by fluorescence measurements (see Figure S2 in the Supporting Information). It was found that, in the absence of target DNA, only a very small fluorescence response could be obtained. The addition of target DNA could induce an obvious fluorescence signal, further providing support for the response mechanism that the target DNA triggers the catalytic assembly of HP1 and HP2 for the execution of the subsequent strand displacement reaction. Control experiments performed in the absence of HP1 or HP2 resulted in nearly the same level of background signal.

Optimization of assay conditions

In order to achieve the best sensing performance, the corresponding experimental conditions including the concentration of immobilized duplex DNA, the reaction temperature, and the reaction time for the CHA were optimized (Figure 3). The immobilization concentration of duplex DNA on the electrode was firstly examined on the basis of the electrochemical re-

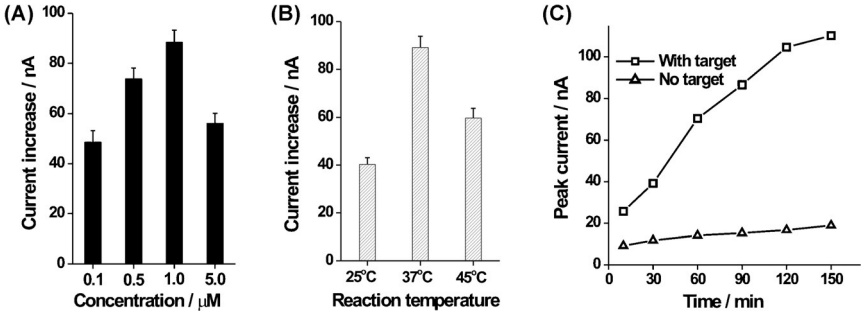

Figure 3. (A) Influence of immobilization concentration of duplex DNA on the electrochemical response toward 1 nM target DNA detection. The duplex DNA was prepared with the hybridization of I-DNA and 1.5 times the concentration of B-DNA. The used duplex DNA concentration corresponded to the I-DNA concentration. (B) Optimization of the reaction temperature for detection of 1 nM target DNA. The current increase in (A) and (B) indicates the electrochemical response difference in the presence and absence of target DNA. (C) The time responses of the fabricated electrochemical DNA biosensor in the presence or absence of 1 nM target DNA, respectively.

sponse toward target DNA. The duplex DNA was prepared with the hybridization of I-DNA and B-DNA. It was found that a concentration of 1 μM (corresponding to 1 μM I-DNA) of immobilized duplex DNA could achieve the best electrochemical response when compared with those at other concentrations (Figure 3A). A higher immobilization concentration of duplex DNA would increase the assembly density, but it may restrict the displacement efficiency for the formation of DNA 3WJ on the electrode surface owing to steric hindrance. The reaction temperature of 37 °C resulted in a better electrochemical response than that at the other two temperatures tested (Figure 3B). The time dependence of the CHA is shown in Figure 3C. It was found that the electrochemical signal increased with increasing incubation time before reaching saturation after 2 h in the presence of target DNA, and only a weak peak current increase was observed in the absence of target DNA. The optimized time for CHA was determined as 2 h.

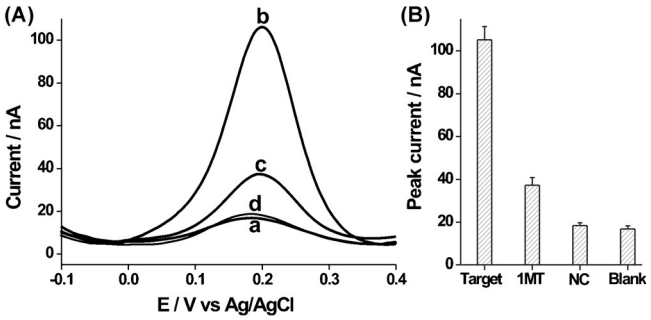

Figure 5. (A) DPV responses toward the blank (a) and three DNA sequences comprising the complementary target DNA (TD) (b), single-base mismatched DNA (1MT) (c), and non-complementary DNA (NC) (d). The concentrations of the various DNA sequences were all 1 nM. (B) Bar chart of the DPV responses toward various DNA sequences. Error bars represent standard deviations of measurements ($n=3$).

Detection sensitivity of the developed DNA biosensor

To further confirm the ability of the proposed biosensor to sensitively detect target DNA, a series of different concentrations of target DNA ranging from 0 to 10 nM were used for measurement (Figure 4A). The electrochemical intensity was observed to increase with increasing concentration of target DNA, indicating that the CHA-induced formation of DNA 3WJ on the electrode surface was highly dependent on the concentration of target DNA. A good linear relationship between the DPV peak current and the logarithmic value of the target DNA concentration ranging from 1 pM to 1 nM was obtained with a correlation coefficient of 0.9971 (Figure 4B). The detection limit, which is defined as 3 times the standard deviation of the background, was about 0.5 pM. This detection limit is better than or comparable to those reported by using CHA for target DNA detection.[9b,f,g]

Selectivity, stability, and regeneration of the developed DNA biosensor

The specificity of the developed CHA-3WJ strategy was further investigated by using three kinds of DNA sequences, including complementary target DNA (TD), single-base mismatched DNA (1MT), and non-complementary DNA (NC) (Figure 5). The DPV peak current response toward 1MT was about 35.4% of that for perfect target DNA at the same concentration, while the NC showed almost the same response as the blank solution. To further evaluate the practical utility of the proposed biosensor, we investigated the detection of target DNA spiked in a relatively complex biological matrix (1% human urine sample). Comparable responses were obtained for the detection of target DNA in both buffer and diluted urine sample (Figure S3, Supporting Information), indicating the potential for the application in a relatively complex biological sample. The stability for the duplex DNA-modified electrode has also been checked. Three independent experiments demonstrated that the duplex DNA-modified electrode could retain about 93.6% of its initial response toward target DNA after its storage at 4 °C for 10 days, indicating a relatively robust stability of the modified electrode. Furthermore, the fabricated DNA biosensor could be regenerated for target DNA detection, which was conducted by the dehybridization in hot water (80 °C) for 10 min. As shown in Figure S4 in the Supporting Information, the regenerated I-DNA-only modified electrode could be directly used for the effective detection of target DNA even after regeneration for three times. Furthermore, the conventional CHA-induced toehold activation strategy was designed for the DNA biosensor fabrication, as illustrated in Figure S5A. It could be seen from Figure S5B that the original background signal in the absence of target DNA (TD2) was larger than that of the proposed CHA-3WJ strategy. Moreover, the fabricated DNA biosensor by the conventional CHA-induced toehold activation strategy was not beneficial for the regeneration experiments. After the dehybridi-

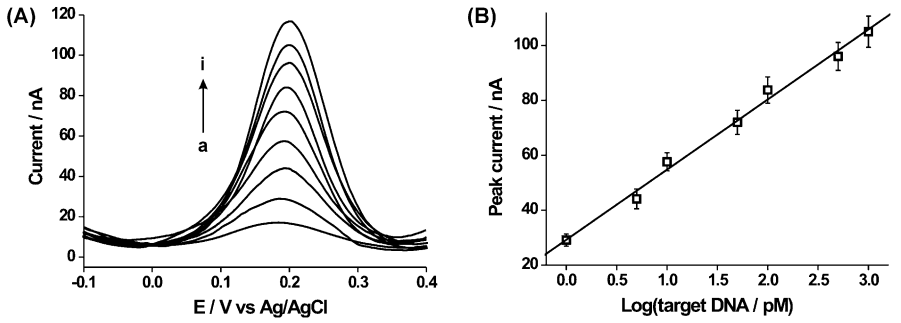

Figure 4. (A) DPV responses corresponding to the analysis of different concentrations of target DNA. The concentrations of target DNA for the curves (a) to (i) are: (a) 0 M, (b) 1 pM, (c) 5 pM, (d) 10 pM, (e) 50 pM, (f) 100 pM, (g) 500 pM, (h) 1 nM, (i) 10 nM. (B) The linear relationship between the DPV peak current and the logarithmic value of the target DNA concentration. Error bars represent standard deviations of measurements ($n=3$).

zation process, the regenerated I-DNA-only modified electrode could not be directly used for the TD2 detection owing to a large background response induced by the direct hybridization between the I-DNA-only modified electrode and the exposed domain **b** in HP3.

Detection versatility of the developed DNA biosensor

Furthermore, the proposed CHA-3WJ strategy could be developed as a versatile approach for the detection of virtually any DNA sequence (Figure 6A). For this purpose, an additional nucleic acid hairpin structure (HP5) that could recognize a new nucleic acid sequence (TD3) was introduced into the system. HP5 was generated by extending the 5′-end of TD1 to form a hairpin loop where the domain **a** of HP5 is occluded by its complementary domain **a***. Therefore, HP5 should be catalytically inactive. When the TD3 is present, it hybridizes with the loop of HP5, forming a rigid duplex and disrupting the stem formed by domain **a** and **a***. The exposed domain **a** of HP5 thereby serves as a toehold for initiating the assembly between HP1 and HP2, and then for the subsequent strand displacement reaction on the electrode surface to form DNA 3WJ. With increasing concentration of TD3, the electrochemical response increased (Figure 6B). Again, a low background signal could be observed in the absence of the target nucleic acid sequence. The BRCA1 breast cancer gene was further chosen as a model target to demonstrate the generalization of the fabricated DNA biosensor with the use of a nucleic acid hairpin structure (HP6) as a signal transducer. It could be seen from Figure S6A that the DPV peak current increased with increasing TD4-BRCA1 concentration. Also, a low background response could be only obtained in the absence of target. The selectivity of the versatile DNA biosensor was also demonstrated and is shown in Figure S6B. The electrochemical response for the single-base mismatched DNA (1MT-BRCA1) was 43.6% of that for the perfect target DNA.

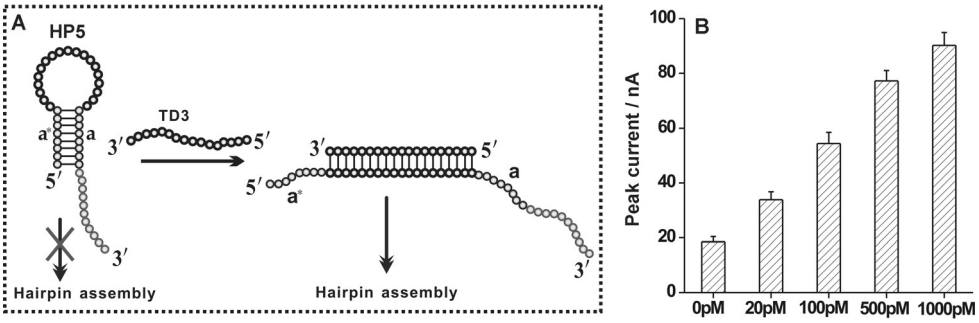

Figure 6. (A) Schematic representation of the general DNA sensing platform by using a pre-designed hairpin structure (HP5) as a signal transducer. (B) Bar chart of DPV responses obtained for the detection of different concentrations of target DNA3 (TD3). The error bars represent the standard deviation of three repetitive measurements.

Conclusions

The CHA-3WJ strategy was fully developed for the sensitive and enzyme-free electrochemical detection of target DNA, in which the CHA was ingeniously manipulated as a dual-functional module for the signal amplification and the induced formation of DNA 3WJ on the electrode surface. The current strategy offers distinct advantages of simplicity in probe design and biosensor fabrication, sensitivity, and enzyme-free operation. The sensor could also be regenerated for target DNA detection. Furthermore, it should be fairly easy to extend this strategy for the detection of a wide spectrum of analytes. The currently proposed strategy could further achieve the effective regulation of a DNA strand displacement reaction and thus constitutes a promising approach for future applications in bioanalysis or DNA nanotechnology.

Experimental Section

Materials and chemicals

Tris(2-carboxyethyl)phosphine (TCEP) and 6-mercapto hexanol (MCH) were purchased from Sigma–Aldrich (St. Louis, MO, USA). The HPLC-purified oligonucleotides were purchased from Sangon Biotech. Co., Ltd. (Shanghai, China) and are listed in Table S1 in the Supporting Information. All other chemicals used were of analytical reagent grade. The urine samples were obtained from healthy volunteers and filtered through a 0.2 mm membrane to remove any particulate matters.

Apparatus

All electrochemical measurements were carried out by using a CHI 660D electrochemical workstation (CH Instruments, Shanghai, China) at room temperature. A conventional three-electrode system was used, which comprised a gold working electrode (2 mm diameter), a platinum wire auxiliary electrode, and an Ag/AgCl reference electrode. Fluorescence measurements were performed using a Hitachi F-4600 spectrofluorimeter at a scan rate of 1200 nm min^{-1} (Tokyo, Japan). The excitation wavelength was set to 490 nm and the 24 photomultiplier voltage was 700 V.

Electrode pretreatment

The gold electrode was cleaned by immersion in a freshly prepared piranha solution (a 3:1 v/v mixture of concentrated H_2SO_4 and 30% H_2O_2) for 20 min, followed by a thorough rinsing with ultrapure water. The electrode was then polished on a microcloth (Shanghai Chenhua Inc., China) with 50 nm alumina slurry to obtain a mirror surface, followed by sonication in acetone and ultrapure water for 5 min each, to remove residual alumina powder. The well-polished electrode was then subjected to electrochemical pretreatment by cycling the potential between −0.2 and 1.5 V in H_2SO_4 (0.5 M) at a scan rate of 100 mV s^{-1} until a stable cyclic voltammogram was obtained. The cleaned electrode was then allowed to dry at room temperature.

Immobilization of duplex DNA on the electrode surface

Each DNA solution was heated to 95 °C for 5 min and then allowed to cool to room temperature before use. The duplex DNA probe

was firstly prepared by mixing the same volume of 1 μM I-DNA and 1.5 μM B-DNA in 10 mM PBS (0.2 M NaCl, 10 mM TCEP, pH 7.9). Then the electrode was incubated into the above DNA duplex probe solution for 12 h at room temperature, thoroughly rinsed with ultrapure water, and dried. The electrode was subsequently immersed in 1 mM MCH solution for 1 h to remove nonspecifically adsorbed DNA.

Catalytic hairpin assembly-programmed DNA three-way junction

The target DNA-catalyzed hairpin assembly was carried out by adding different concentrations of target DNA into 50 μL of 10 mM PBS buffer (0.2 M NaCl, pH 7.9) containing 1 μM HP1 and 1 μM HP2 and incubation for 2 h at 37 °C. Then the I-DNA and B-DNA modified electrode was incubated with the above solution for another 2 h at 37 °C. Subsequently, the electrodes were taken out and rinsed with buffer and ultrapure water for further electrochemical measurements. For the operation of the general DNA sensing strategy, HP5 and different concentrations of target DNA3 (TD3) or HP6 and BRCA1 breast cancer-related DNA sequences were added into 50 μL of 10 mM PBS buffer (0.2 M NaCl, pH 7.9) containing 1 μM HP1 and 1 μM HP2 for 2 h at 37 °C. The other operation procedures were the same as described above.

Electrochemical measurements

Differential pulse voltammetric (DPV) results were recorded in 10 mM PBS buffer (200 mM KNO_3, pH 7.9) with a potential window from 0.4 V to −0.1 V, a pulse amplitude of 50 mV, and a pulse period of 0.2 s. The electrochemical impedance spectra (EIS) were recorded in 1 mM $[Fe(CN)_6]^{3-/4-}$and 0.1 M KNO_3 with the frequency ranging from 0.1 Hz to 10 kHz. Before measurements, the electrolyte solution was thoroughly purged with high-purity nitrogen for about 20 min.

Acknowledgements

This work was funded by the National Natural Science Foundation of China (Nos. 21475072, 21005043), the Natural Science Foundation of Shandong Province of China (Nos. ZR2015JL007, ZR2014M019), the Basic Research Program of Qingdao (No. 13-1-4-214-jch) and the Science Foundation of China Postdoctor (No. 2012M511537).

Keywords: DNA biosensors · DNA three-way junction · electrochemical detection · strand displacement · target catalyzed hairpin assembly

[1] a) A. Sassolas, B. D. Leca-Bouvier, L. J. Blum, *Chem. Rev.* **2008**, *108*, 109–139; b) N. K. Navani, Y. Li, *Curr. Opin. Chem. Biol.* **2006**, *10*, 272–281; c) C. L. Sawyers, *Nature* **2008**, *452*, 548–552; d) A. P. F. Turner, *Chem. Soc. Rev.* **2013**, *42*, 3184–3196; e) Q. Wang, Y. Ding, L. Wang, J. Ni, Z. Yu, H. Lin, F. Gao, *Chem. Asian J.* **2013**, *8*, 1455–1462.

[2] a) J. Lei, H. Ju, *Chem. Soc. Rev.* **2012**, *41*, 2122–2134; b) L. Qiu, L. Qiu, Z. Wu, G. Shen, R. Yu, *Anal. Chem.* **2013**, *85*, 8225–8231; c) F. Gao, J. Lei, H. Ju, *Chem. Commun.* **2013**, *49*, 4006–4008.

[3] a) H. Ji, F. Yan, J. Lei, H. Ju, *Anal. Chem.* **2012**, *84*, 7166–7171; b) X. Zuo, F. Xia, Y. Xiao, K. W. Plaxco, *J. Am. Chem. Soc.* **2010**, *132*, 1816–1818; c) R. Duan, X. Zuo, S. Wang, X. Quan, D. Chen, Z. Chen, L. Jiang, C. Fan, F. Xia, *J. Am. Chem. Soc.* **2013**, *135*, 4604–4607.

[4] a) Y. Li, Y. D. Tseng, S. Y. Kwon, L. D'Espaux, J. S. Bunch, P. L. McEuen, D. Luo, *Nat. Mater.* **2004**, *3*, 38–42; b) R. P. Goodman, I. A. T. Schaap, C. F. Tardin, C. M. Erben, R. M. Berry, C. F. Schmidt, A. J. Turberfield, *Science* **2005**, *310*, 1661–1665; c) D. Shu, Y. Shu, F. Haque, S. Abdelmawla, P. Guo, *Nat. Nanotechnol.* **2011**, *6*, 658–667; d) N. C. Seeman, N. R. Kallenbach, *Annu. Rev. Biophys. Biomol. Struct.* **1994**, *23*, 53–86; e) X. Chen, *J. Am. Chem. Soc.* **2012**, *134*, 263–271.

[5] M. Probst, D. Wenger, S. M. Biner, R. Häner, *Org. Biomol. Chem.* **2012**, *10*, 755–759.

[6] a) I. T. Seemann, V. Singh, M. Azarkh, M. Drescher, J. S. Hartig, *J. Am. Chem. Soc.* **2011**, *133*, 4706–4709; b) J. M. Thomas, B. Chakraborty, D. Sen, H. Z. Yu, *J. Am. Chem. Soc.* **2012**, *134*, 13823–13833; c) B. Ge, Y. C. Huang, D. Sen, H. Z. Yu, *Angew. Chem. Int. Ed.* **2010**, *49*, 9965–9967; *Angew. Chem.* **2010**, *122*, 10161–10163; d) J. Zhu, L. Zhang, Z. Zhou, S. Dong, E. Wang, *Anal. Chem.* **2014**, *86*, 312–316.

[7] a) F. Li, Y. Lin, X. C. Le, *Anal. Chem.* **2013**, *85*, 10835–10841; b) C. Zong, J. Wu, M. Liu, L. Yang, L. Liu, F. Yan, H. Ju, *Anal. Chem.* **2014**, *86*, 5573–5578; c) J. M. Thomas, H. Z. Yu, D. Sen, *J. Am. Chem. Soc.* **2012**, *134*, 13738–13748; d) J. Zhu, L. Wang, W. Jiang, *Chem. Commun.* **2015**, *51*, 2903–2906.

[8] a) Q. Li, Y. D. Wang, G. L. Shen, H. Tang, R. Q. Yu, J. H. Jiang, *Chem. Commun.* **2015**, *51*, 4196–4199; b) R. M. Kong, X. B. Zhang, L. L. Zhang, Y. Huang, D. Q. Lu, W. Tan, G. L. Shen, R. Q. Yu, *Anal. Chem.* **2011**, *83*, 14–17; c) H. Zhou, S. J. Xie, S. B. Zhang, G. L. Shen, R. Q. Yu, Z. S. Wu, *Chem. Commun.* **2013**, *49*, 2448–2450; d) B. Liu, J. Chen, Q. Wei, B. Zhang, L. Zhang, D. Tang, *Biosens. Bioelectron.* **2015**, *69*, 241–248.

[9] a) C. Jung, A. D. Ellington, *Acc. Chem. Res.* **2014**, *47*, 1825–1835; b) B. Li, A. D. Ellington, X. Chen, *Nucleic Acids Res.* **2011**, *39*, e110; c) K. Scida, B. Li, A. D. Ellington, R. M. Crooks, *Anal. Chem.* **2013**, *85*, 9713–9720; d) B. Li, Y. Jiang, X. Chen, A. D. Ellington, *J. Am. Chem. Soc.* **2012**, *134*, 13918–13921; e) K. Quan, J. Huang, X. Yang, Y. Yang, L. Ying, H. Wang, Y. He, K. Wang, *Chem. Commun.* **2015**, *51*, 937–940; f) A. X. Zheng, J. Li, J. R. Wang, X. R. Song, G. N. Chen, H. H. Yang, *Chem. Commun.* **2012**, *48*, 3112–3114; g) J. Huang, X. Su, Z. Li, *Anal. Chem.* **2012**, *84*, 5939–5943.

[10] a) Y. Jiang, B. Li, J. N. Milligan, S. Bhadra, A. D. Ellington, *J. Am. Chem. Soc.* **2013**, *135*, 7430–7433; b) C. Li, Y. Li, X. Xu, X. Wang, Y. Chen, X. Yang, F. Liu, N. Li, *Biosens. Bioelectron.* **2014**, *60*, 57–63.

[11] a) Z. Shen, S. Nakayama, S. Semancik, H. O. Sintim, *Chem. Commun.* **2012**, *48*, 7580–7582; b) S. Tang, P. Tong, H. Li, F. Gu, L. Zhang, *Biosens. Bioelectron.* **2013**, *41*, 397–402.

Manuscript received: July 1, 2015
Accepted Article published: July 14, 2015
Final Article published: August 6, 2015